TABLE 1. Differentially expressed predominant genes detected in spinal anterior horn or spinal motor neurons from SOD1 mutant mice and sporadic ALS patients

Analysis object	SOD1 G93A mutant mice[5,13] spinal anterior horn	SALS patients[7,18] spinal anterior horn	SALS patients[9] spinal anterior horn	SALS patients[9] spinal motor neuron
Analysis method	cDNA microarray 30/1176	Molecular indexing 46/entire mRNA	cDNA microarray 37/4845	cDNA microarray 52/4845
Upregulated genes in ALS	TNF-α*† JAK3† cathepsin D serine protease inhibitor (SPI) 2-4	dorfin* TAFII30* neugrin*	KIAA0231 fibrinogen A a polypeptide presenilin 1 ephrin A1	death receptor 5 (DR5)* cyclin A1, cyclin C*, ephrin A1* caspase 1, caspase 3, caspase 9 acetyl-coenzyme A transporter*, NF-κB
	cystatin C precursor		transcription factor NF-Atc	ciliary neurotrophic factor (CNTF)
	CD68*, CD147 clusterin		SH3-binding protein 2 integrin alpha E precursor (ITGAE)	hepatocyte growth factor (HGF) glial cell line–derived neurotrophic factor (GDNF)
	caspase-1*†, caspase-3 GFAP*, vimentin Bcl-xL		cysteine dioxygenase, type 1	KIAA0231* glutamate receptor subunit 2 (GLUR-2) interleukin-1 receptor antagonist TNF receptor-associated factor 6 (TRAF6)
	c-fos, junD 7/1176 XIAP	38/entire mRNA metallothionein-3*	8/4845 glutamate receptor, metabotropic 6	144/4845 dynactin 1 (p150)*, TRK-C*, midkine, musashi 1
Downregulated genes in ALS	GABAA-receptor-α1	MRP8*	cholecystokinin A receptor	microtubule-associated protein 1A, 4
		ubiquitin-like protein 5*	signal recognition particle 14kD syntaxin 1B sex-determining region Y (SRY)-box 11	microtubule-associated protein tau early growth response 3 (EGR3)* BCL2-antagonist/killer 1 (Bak)*
				cellular retinoic acid-binding protein 1 (CRABP1)* retinoic acid receptor-α

Principal genes showing expression changes of 3.0-fold increase and 0.3-fold decrease are listed. Fold-change is calculated by dividing the fluorescence signals of each ALS sample by those of control samples. *Gene expression changes were confirmed by other methods such as reverse transcription–polymerase chain reaction (RT-PCR) or in situ hybridization. †Genes upregulated in 11-week-old mice.

the result that at 14 weeks of age XIAP mRNA downregulation occurred in the spinal cords of mutant SOD1 mice (TABLE 1) since XIAP is a direct inhibitor of caspase-3, -7, and -9.[14]

DISCOVERY OF NOVEL GENES ASSOCIATED WITH ALS PATHOGENESIS

To identify genes differentially expressed in the anterior horn tissues of the human SALS spinal cord, we adopted molecular indexing, a modified version of the differential display.[6] The entire mRNA population is identified and displayed by 3$'$ end cDNA fragments generated by class IIS restriction enzyme digestion and PCR.[6] Accordingly, molecular indexing provides a significant advantage in expression analysis for unknown genes. Among 84 fragments differentially expressed in SALS cloned in the first screening procedure, we noticed a fragment with an unknown sequence overexpressed in SALS spinal cords. We cloned it using RACE methods and named it dorfin (double ring-finger protein)[7] (TABLE 1).

Dorfin contains a RING-IBR (in between ring finger) domain at its N terminus and mediated ubiquitin ligase (E3) activity.[7] Interestingly, dorfin is predominantly localized and overexpressed in the ubiquitinated neuronal hyaline inclusion bodies found in the motor neurons of SALS patients as well as FALS patients with a SOD1 mutation and of mutant SOD1-transgenic mice.[15,16] An *in vitro* assay revealed that dorfin physically bound and ubiquitylated various SOD1 mutants and enhanced their degradation, and that its overexpression protected neural cells against the toxic effects of mutant SOD1 and reduced SOD1 inclusions.[15,17] These findings suggest that dorfin, an E3 ligase, may play some protective role in the pathogenesis of FALS and SALS via the ubiquitylation and degradation of its substrates, mutant SOD1, and others yet to be identified.

Besides dorfin, we have detected 30-kDa TATA binding protein-associated factor (TAFII30) and neugrin as upregulated genes in the SALS spinal cord[18] (TABLE 1). On the other hand, metallothionein-3, macrophage-inhibiting factor-related protein-8 (MRP-8) and ubiquitin-like protein 5 were downregulated in their expression[18] (TABLE 1).

MOTOR NEURON-SPECIFIC GENE EXPRESSION PROFILE IN SALS

As noted above, even using spinal anterior horn tissues consisting of heterogeneous cell types including motor neurons and glial cells as starting materials, gene expression studies have successfully shed light on the genes related to the pathogenesis of FALS and SALS.[5,7,18] However, the constitution
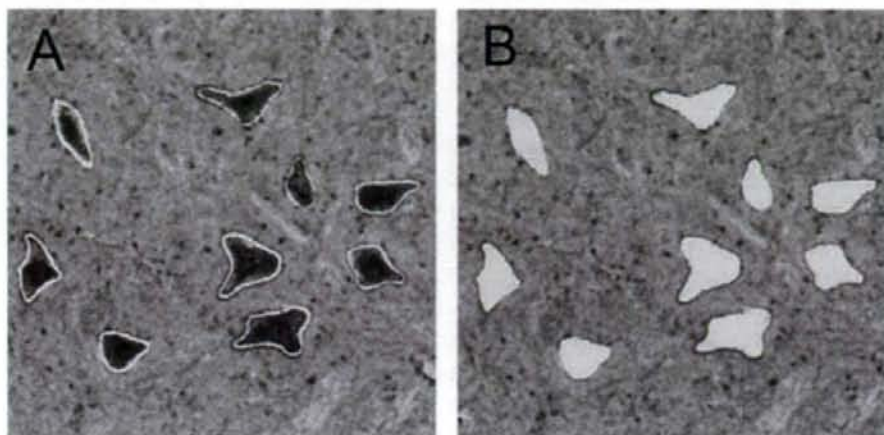
FIGURE 1. Laser microdissection of motor neurons in spinal anterior horn. sections were stained with hematoxylin and margins of motor neurons were dissected by the laser beam (**A**); motor neurons were isolated from slides by laser pressure catapulting (**B**).

of spinal anterior horn tissues is overwhelmingly dominated by glial cells in comparison with motor neurons. Furthermore, in the lesions of ALS spinal cords, there are reduced numbers of motor neurons with glial cell proliferation. When the genes display a dramatic change of expression in ALS motor neurons, they can be detected (TABLE 1) even by using spinal anterior horn tissues. In fact, we have successfully cloned dorfin overexpressed in SALS motor neurons[7] as described above. However, a small change of gene expression in motor neurons might be masked by a large quantity of glial cells and such genes might be those we are seeking as the essential ones for ALS pathomechanisms. The technologies of laser capture microdissection have been developed to provide a reliable method of procuring pure populations of cells from specific microscopic regions of tissue sections under direct visualization.[8,19] The pulsed laser microbeam cut precisely around the targeted motor neurons in the spinal anterior horn (FIG. 1). Each laser-isolated specimen was subsequently transferred to the cap of a PCR tube that was activated by laser pulses.

Using this technology combined with T7 RNA polymerase-based RNA amplification[20] and cDNA microarrays, we have obtained motor neuron-specific gene expression profiles of SALS patients[9] (TABLE 1). Simultaneously, we also conducted conventional gene expression analysis using spinal anterior horn tissues and validated the differential characteristics[9] (TABLE 1). As a result, spinal motor neurons showed a gene expression profile distinct from that of spinal anterior horn tissues (TABLE 1). Of the genes examined 3% (144/4845) were downregulated and 1% (52/4845) were upregulated in motor neurons. Downregulated genes included those associated with cytoskeleton/axonal

transport, transcription, and cell surface antigens/receptors such as dynactin 1, microtubule-associated proteins, and early growth response 3 (EGR3). In contrast, cell death-associated genes were mostly upregulated. Promoters for a cell death pathway, death receptor 5 (DR5), cyclins A1 and C, and caspases-1, -3, and -9, were upregulated as were cell death inhibitors, acetyl-CoA transporter, and NF-κB (TABLE 1). Moreover, neuroprotective neurotrophic factors such as ciliary neurotrophic factor (CNTF), hepatocyte growth factor (HGF), and glial cell line-derived neurotrophic factor (GDNF) were upregulated. However, inflammation-related genes such as those belonging to the cytokine family were not significantly upregulated in SALS motor neurons.

One of the interesting genes downregulated in motor neurons was dynactin 1, recently identified as a causative gene for human motor neuron disease.[21–23] Other motor proteins including the kinesin family responsible for antegrade axonal transport and dyneins for retrograde axonal transport were not changed significantly, but the expression levels of microtubule-associated proteins (MAPs) 1A, 4, and tau were reduced (TABLE 1). The impairment of axonal transport is thought to be an early event in motor neuron degeneration, and the protein levels of MAPs 1A and tau have especially been reported to decrease well before the onset of symptoms in mutant SOD1 transgenic mice also.[24]

As shown in the examples of MAPs 1A and tau, gene expression profiles of SALS patients may share some features with those of SOD1 mutant mice. However, taking into account our overall differential gene expression profiles between mice and humans drawn from spinal anterior horn tissues (TABLE 1), the disease in transgenic mouse may mimic but not be identical to the pathophysiology in human SALS. Consequently, we should be cautious about applying the research results of the pathophysiological process or therapeutic strategy obtained from SOD1 mutant mice to human SALS patients.

Seen in this light, the gene expression data of SALS motor neurons obtained by our analysis are of particular value and contribute a starting point for clarifying the pathomechanisms of a great many more SALS than FALS. At present, it is not easy to determine the genes of primary pathological significance from a total of 144 downregulated and 52 upregulated genes in SALS motor neurons. The primary molecular events should occur in the preclinical phase of the disease. Unlike the case of mice, it is impossible to obtain human spinal cord specimens at a preclinical stage. However, even in postmortem tissue, some motor neurons remain intact and have not yet started to degenerate. From this standpoint, a detailed investigation of the gene expression level, particularly in motor neurons, verified to be intact by reliable neurodegenerative markers would lead to the successful detection of genes related to primary molecular events. Detecting such genes would provide a first step toward a new molecular targeted therapy for SALS by developing animal or cell models mimicking those upstream and primary molecular events determined in human SALS patients.

INTEGRATED RESEARCH FOR NEURODEGENERATION
AND TUMORIGENESIS

Among the genes in which we have detected an alteration in their expression in SOD1 mutant mice or SALS patients, a number of them are well known to be related to tumorigenesis rather than neurodegeneration (TABLE 1). Evidence has been steadily accumulating for the existence of many common molecular pathways between neurodegeneration and tumorigenesis.[25] Based on the concept of "Integrated Molecular Medicine for Neuronal and Neoplastic Disorders" proposed by The 21st Century Center of Excellence (COE) Program at Nagoya University,[26] the contribution of these tumor-related genes to the molecular mechanism of ALS should be clarified to advance our understanding of this devastating disease.

ACKNOWLEDGMENTS

REFERENCES

1. INCE, P.G., J. LOWE & P.J. SHAW. 1998. Amyotrophic lateral sclerosis: current issues in classification, pathogenesis and molecular pathology. Neuropathol. Appl. Neurobiol. **24:** 104–117.
2. SIDDIQUE, T. & H.X. DENG. 1996. Genetics of amyotrophic lateral sclerosis. Hum. Mol. Genet. **5:** 1465–1470.
3. TAKEUCHI, H., Y. KOBAYASHI, S. ISHIGAKI, *et al*. 2002. Mitochondrial localization of mutant superoxide dismutase 1 triggers caspase-dependent cell death in a cellular model of familial amyotrophic lateral sclerosis. J. Biol. Chem. **277:** 50966–50972.
4. MALASPINA, A. & J. de Belleroche. 2004. Spinal cord molecular profiling provides a better understanding of amyotrophic lateral sclerosis pathogenesis. Brain Res. Brain Res. Rev. **45:** 213–229.
5. YOSHIHARA, T., S. ISHIGAKI, M. YAMAMOTO, *et al*. 2002. Differential expression of inflammation- and apoptosis-related genes in spinal cords of a mutant SOD1 transgenic mouse model of familial amyotrophic lateral sclerosis. J. Neurochem. **80:** 158–167.
6. KATO, K. 1995. Description of the entire mRNA population by a 3′ end cDNA fragment generated by class IIS restriction enzymes. Nucleic Acids Res. **23:** 3685–3690.

7. NIWA, J., S. ISHIGAKI, M. DOYU, *et al.* 2001. A novel centrosomal ring-finger protein, dorfin, mediates ubiquitin ligase activity. Biochem. Biophys. Res. Commun. **281:** 706–713.

8. BOHM, C., D. NEWRZELLA & O. SORGENFREI. 2005. Laser microdissection in CNS research. Drug Discov. Today **10:** 1167–1174.

9. JIANG, Y.M., M. YAMAMOTO, Y. KOBAYASHI, *et al.* 2005. Gene expression profile of spinal motor neurons in sporadic amyotrophic lateral sclerosis. Ann. Neurol. **57:** 236–251.

10. HALL, E.D., J.A. OOSTVEEN & M.E. GURNEY. 1998. Relationship of microglial and astrocytic activation to disease onset and progression in a transgenic model of familial ALS. Glia **23:** 249–256.

11. GRAY, F., H. ADLE-BIASSETTE, F. BRION, *et al.* 2000. Neuronal apoptosis in human immunodeficiency virus infection. J. Neurovirol. **6:** S38–S43.

12. MINGHETTI, L. & G. LEVI. 1998. Microglia as effector cells in brain damage and repair: focus on prostanoids and nitric oxide. Prog. Neurobiol. **54:** 99–125.

13. ANDO, Y., Y. LIANG, S. ISHIGAKI, *et al.* 2003. Caspase-1 and -3 mRNAs are differentially upregulated in motor neurons and glial cells in mutant SOD1 transgenic mouse spinal cord: a study using laser microdissection and real-time RT-PCR. Neurochem. Res. **28:** 839–846.

14. ISHIGAKI, S., Y. LIANG, M. YAMAMOTO, *et al.* 2002. X-linked inhibitor of apoptosis protein is involved in mutant SOD1-mediated neuronal degeneration. J. Neurochem. **82:** 576–584.

15. NIWA, J., S. ISHIGAKI, N. HISHIKAWA, *et al.* 2002. Dorfin ubiquitylates mutant SOD1 and prevents mutant SOD1-mediated neurotoxicity. J. Biol. Chem. **277:** 36793–36798.

16. ISHIGAKI, S., N. HISHIKAWA, J. Niwa, *et al.* 2004. Physical and functional interaction between Dorfin and Valosin-containing protein that are colocalized in ubiquitylated inclusions in neurodegenerative disorders. J. Biol. Chem. **279:** 51376–51385.

17. TAKEUCHI, H., J. NIWA, N. Hishikawa, *et al.* 2004. Dorfin prevents cell death by reducing mitochondrial localizing mutant superoxide dismutase 1 in a neuronal cell model of familial amyotrophic lateral sclerosis. J. Neurochem. **89:** 64–72.

18. ISHIGAKI, S., J. NIWA, T. YOSHIHARA, *et al.* 2000. Two novel genes, human neugrin and mouse m-neugrin, are upregulated with neuronal differentiation in neuroblastoma cells. Biochem. Biophys. Res. Commun. **279:** 526–533.

19. LUO, L., R.C. SALUNGA, H. GUO, *et al.* 1999. Gene expression profiles of laser-captured adjacent neuronal subtypes. Nat. Med. **5:** 117–122.

20. Van GELDER, R.N., M.E. VON ZASTROW, A. YOOL, *et al.* 1990. Amplified RNA synthesized from limited quantities of heterogeneous cDNA. Proc. Natl. Acad. Sci. USA **87:** 1663–1667.

21. PULS, I., C. JONNAKUTY, B.H. LAMONTE BH, *et al.* 2003. Mutant dynactin in motor neuron disease. Nat. Genet. **33:** 455–456.

22. PULS, I., S.J. OH, C.J. SUMNER, *et al.* 2005. Distal spinal and bulbar muscular atrophy caused by dynactin mutation. Ann. Neurol. **57:** 687–694.

23. Levy, J.R., C.J. SUMNER, J.P. Caviston, *et al.* 2006. A motor neuron disease-associated mutation in p150Glued perturbs dynactin function and induces protein aggregation. J. Cell. Biol. **172:** 733–745.

24. FARAH, C.A., M.D. NGUYEN, J.P. JULIEN, *et al*. 2003. Altered levels and distribution of microtubule-associated proteins before disease onset in a mouse model of amyotrophic lateral sclerosis. J. Neurochem. **84:** 77–86.
25. WAZA, M., H. ADACHI, M. KATSUNO, *et al*. 2005. 17-AAG, an Hsp90 inhibitor, ameliorates polyglutamine-mediated motor neuron degeneration. Nat. Med. **11:** 1088–1095.
26. THE 21ST CENTURY COE PROGRAM: Integrated Molecular Medicine for Neuronal and Neoplastic Disorders. http://www.nagoya-u.ac.jp/coemed/.

Clinicopathologic features of nonsystemic vasculitic neuropathy and microscopic polyangiitis-associated neuropathy: A comparative study

M. Sugiura, H. Koike, M. Iijima, K. Mori, N. Hattori, M. Katsuno, F. Tanaka, G. Sobue *

Department of Neurology, Nagoya University Graduate School of Medicine, Nagoya 466-8550, Japan

Abstract

Objective: To compare clinicopathologic findings in nonsystemic vasculitic neuropathy (NSVN) and microscopic polyangiitis-associated neuropathy (MPAN).

Methods: Patients clinicopathologically confirmed to have NSVN ($n=23$) or MPAN ($n=40$) were compared with respect to clinical, electrophysiologic, and histopathologic features.

Results: Clinical features of neuropathy such as initial symptoms, progression, and distribution of sensory and motor deficits were similar in both groups, while functional compromise was greater in MPAN than NSVN. Abnormalities of laboratory data including those reflecting severity and extent of inflammation such as C-reactive protein were more conspicuous in MPAN than NSVN. Perinuclear anti-neutrophil cytoplasmic antibodies (p-ANCA) were positive in two-thirds of patients with MPAN but negative in all NSVN. Electrophysiologic and histopathologic findings indicated axonal neuropathy in both groups, whereas the reduction of compound muscle action potentials in the tibial nerve and sensory nerve action potentials in the median nerve was significantly more profound in MPAN than NSVN. As for the epineurial perivascular infiltration, frequencies of cell-specific markers for T lymphocytes, macrophages, and B lymphocytes among cells infiltrating the vasculitic lesions were essentially similar between groups.

Conclusions: Clinicopathologic profiles and vascular pathology were similar between NSVN and MPAN but the age at onset, severity, and presence of p-ANCA were clearly different. Further study is needed to clarify the pathogenesis of NSVN and its place in the vasculitic spectrum of diseases.
© 2005 Elsevier B.V. All rights reserved.

Keywords: Nonsystemic vasculitic neuropathy; Microscopic polyangiitis; Sural nerve biopsy

1. Introduction

Vasculitic neuropathy occurs in association with various diseases including systemic lupus erythematosus, rheumatoid arthritis, Sjögren's syndrome, infection, malignant neoplasia, and cryogloblinemia [1]. In addition to vasculitic neuropathies secondarily to these diseases, primary systemic vasculitides including microscopic polyangiitis (MPA), Churg-Strauss syndrome, and Wegener's granulomatosis are known to involve the peripheral nervous system. Finally, vasculitis confined to the peripheral nervous system without systemic manifestations has been reported [2,3]. Subse-

quently, Dyck et al. described 20 patients with vasculitic neuropathy in the absence of other organ involvement [4]. These patients showed few laboratory abnormalities suggesting either systemic inflammation or collagen diseases, lacked nonspecific constitutional symptoms such as fever or weight loss, and had a favorable prognosis [4]. Since then, such vasculitic neuropathy has been known as nonsystemic vasculitic neuropathy (NSVN) and has attracted attention mainly among neurologists. Although NSVN possesses distinctive clinical features, involving only the peripheral nervous system, pathogenesis has remained unknown. In addition, vasculitis in this neuropathy has not been proven pathologically to be confined to the peripheral nervous system, so it might subclinically involve other organs. A related question is whether NSVN has a pathogenesis

* Corresponding author. Tel.: +81 52 744 2385; fax: +81 52 744 2384.
  E-mail address: sobueg@med.nagoya-u.ac.jp (G. Sobue).

distinct from that of systemic vasculitides, especially MPA. MPA, a vasculitis involving small vessels including arterioles, venules, or capillaries [5], originally was considered a subtype of polyarteritis nodosa with rapidly progressive necrotizing glomerulonephritis and sometimes lung hemorrhage [6]; because of frequent renal involvement [5], this disorder has been studied by nephrologists as well as rheumatologists, with far less attention given to its neurologic aspects [5,7]. Since diagnostic criteria for primary vasculitis, such as those of Chapel Hill Consensus Conference [7], have been established mainly by rheumatologists, the nosologic relationship of systemic vasculitides to NSVN has remained obscure.

In this study we compared clinicopathologic features of neuropathy without and with systemic involvement (so-called NSVN and MPA-associated neuropathy: MPAN) to clarify the relationship of NSVN to systemic vasculitic neuropathy.

2. Patients and methods

2.1. Patients

Clinicopathologic findings in consecutive patients with pathologically confirmed NSVN and MPA-associated neuropathy (MPAN) with systemic involvement who were referred to Nagoya University Graduate School of Medicine and performed sural nerve biopsy from 1990 to 2003 were retrospectively compared. In the NSVN group symptoms of vasculitis were confined solely to the peripheral nerves, with no clinical or laboratory evidence of other organ involvement [4]. Laboratory data in this group were normal or only mildly abnormal, without indicating any other underlying disease. Inclusion criteria for the MPAN group were based on the classification proposed by the Chapel Hill Consensus Conference in 1994 [7]. In addition to peripheral nervous system, MPAN group was required to show signs of involvement of other organs such as lung or kidney, or a positive titer for perinuclear anti-neutrophil cytoplasmic antibodies (p-ANCA) for inclusion [5,8]. Signs of a pulmonary-renal syndrome included acute renal insufficiency, hemoptysis, dyspnea, anemia, and alveolar shadowing on the chest radiograph [5]. Presence of vasculitis in the epineurium of sural nerve biopsy specimens was required for inclusion in either group. Vasculitis was defined as previously established [9]. Definite vasculitis was diagnosed if at least one blood vessel was infiltrated by inflammatory cells in association with signs of vascular injury such as fibrinoid necrosis, endothelial cell disruption, fragmentation of the internal elastic lamina, hemorrhage, or acute thrombosis. Probable vasculitis required transmural or perivascular inflammation unaccompanied by vascular destruction, but combined with at least one other supportive finding including vascular thickening, luminal obliteration, recan-

alized thrombus, epineurial neovascularisation, hemosiderin deposits, asymmetric nerve fiber loss, or ongoing Wallerian-like degeneration. Only subjects meeting criteria for definite or probable vasculitis were included in this study. Thus, patients with only perivascular inflammatory cell infiltration were not included. In the MPAN group 33 patients met definite criteria, while 7 met probable criteria. In the NSVN group, 11 patients met definite and 12 met probable criteria. Three patients for each group were clinically suspected as NSVN or MPAN but they did not fulfill the pathologic criteria. Patients with the other small-vessel angiitis such as Churg-Strauss syndrome, Wegener's granulomatosis, malignancy-associated vasculitis, or connective tissue disease-associated vasculitis were excluded. Based on these criteria, 23 patients with NSVN and 40 with MPAN were included.

The functional state of patients was estimated at the peak phase of neuropathy according to the modified Rankin scale [10]: 0, asymptomatic; 1, non-disabling symptoms not interfering with lifestyle; 2, mildly disabling symptoms leading to some restrictions of lifestyle but not interfering with capacity to look after oneself; 3, moderately disabling symptoms significantly interfering with lifestyle or precluding totally independent existence; 4, moderately severe disability precluding independent existence while not requiring constant attention around the clock; and 5, severe disability with total dependency requiring constant attention day and night.

2.2. Electrophysiologic assessment

Motor and sensory nerve conduction studies were performed in all patients before sural nerve biopsy was performed, using a standard method with surface stimulating and recording electrodes [11,12]. Motor conduction was investigated in the median and tibial nerves, with potentials recorded from the abductor pollicis brevis and abductor hallucis brevis muscles, respectively. Sensory conduction was investigated in the median and sural nerves, with potentials recorded at the second digit with ring electrodes and at the ankle, respectively.

2.3. Pathologic assessment of sural nerve specimens

Sural nerve biopsy was performed as described previously prior to initiation of therapy [13–15]. Specimens were divided into two portions. The first was fixed in 2.5% glutaraldehyde in 0.125 M cacodylate buffer (pH 7.4); then most of it was embedded in epoxy resin for morphometric and ultrastructural study. Density of myelinated fibers was assessed in toluidine blue-stained semithin sections using a computer-assisted image analyzer (Luzex FS; Nikon, Tokyo, Japan), and densities of small and large myelinated fibers were calculated as described previously [14–16]. A fraction of the glutaraldehyde-fixed sample was processed for teased-fiber study, in which at least 100 single fibers

were isolated; their pathologic state was assessed microscopically according to criteria described previously [14,17]. The second portion of the specimen was fixed in 10% formalin solution and embedded in paraffin. Sections cut in transverse and longitudinal planes were stained with haematoxylin and eosin or by the Masson trichrome method for conventional observation.

Cases where frozen specimens including a clearly involved vessel could be obtained were subjected to immunohistochemical assessment of infiltrating cells. For each sample, consecutive 4- to 8-μm cryostat sections were cut, fixed in cold acetone, and stained with the following primary antibodies: mouse monoclonal anti-CD45, anti-CD68, anti-CD20, anti-CD4, and anti-CD8. Numbers of CD45-, CD68-, and CD20-positive cells were estimated by projecting each slide through a Lusex FS monitor overlaid with a grid corresponding to a 0.25 mm^2 area of the frozen specimen. Proportions of cells stained for each marker were counted blindly by 2 independent investigators and expressed as a ratio relative to the total number of cells stained with any of the three markers. Ratios of CD4- to CD8-positive cells were also determined. When specimens contained more than one clearly involved vessel, the most intensely infiltrated vessel was evaluated. Variations in estimation between measurements made by the 2 investigators were less than 15% of the mean.

2.4. Statistical analyses

Quantitative data, presented as the mean±S.D., were compared with previously described control values [14,18,19]. Statistical analyses were performed using the χ^2 test or the Mann–Whitney U-test as appropriate. A p value less than 0.05 was considered to indicate significance.

3. Results

3.1. General symptoms

Age at onset was significantly younger in the NSVN group than the MPAN group (58.4 ± 15.3 versus 67.2 ± 8.0 years; $p<0.05$; Table 1). The male to female ratio was 1.6:1 in NSVN and 1.9:1 in MPAN. Nonspecific symptoms, specifically fever, weight loss, skin eruption, arthralgia, and myalgia, respectively were seen in 83%, 43%, 30%, 13% and 13% of MPAN patients; these symptoms were absent in NSVN patients. In the MPAN group, renal involvement was present in 38% of patients, and pulmonary involvement in 28%. Cardiac symptom was evident in 8% of MPAN patients. Ulceration, perforation, or other gastrointestinal lesions caused by vasculitis was seen in 10% of MPAN patients. In NSVN, evidence of involvement of visceral organs was not seen in any patient. No patient in the NSVN group manifested evidence of abnormalities in extraneural sites during the follow up period of 23 ± 15 months.

Table 1
Background of patients with NSVN and MPAN

	NSVN ($n=23$)	MPAN ($n=40$)
Age (years)*	58.4 ± 15.3	67.2 ± 8.0
Sex (M/F)**	14:9 (1.6:1)	26:14 (1.9:1)
Fever	0 (0%)	33 (83%)
Weight loss	0 (0%)	17 (43%)
Skin eruption	0 (0%)	12 (30%)
Arthralgia	0 (0%)	5 (13%)
Myalgia	0 (0%)	5 (13%)
Renal manifestation	0 (0%)	15 (38%)
Pulmonary involvement	0 (0%)	11 (28%)
Cardiac involvement	0 (0%)	3 (8%)
Gastrointestinal involvement	0 (0%)	4 (10%)

Probability was determined with the Mann–Whitney U-test or the χ^2 test as appropriate.
Values are expressed as the number of patients with percentage in the parenthesis or the mean±S.D.
* $p<0.05$.
** Not significant.

3.2. Neuropathic symptoms

The initial symptom of neuropathy was paresthesia or pain in the extremities in 91% of the NSVN group and 85% of the MPAN group, while weakness occurred initially in 9% and 15% in these respective groups (Table 2). Progression of neuropathic symptoms was acute or subacute (occurring within 3 months) in 43% of the NSVN group and in 56% of the MPAN group, while slow progression over 1 year until initiation of therapy was seen in some other members of the respective groups (17% and 11%). The most frequent pattern of neuropathy was that of multiple mononeuropathy, which characterised 78% of NSVN and 80% of MPAN groups. Remaining patients manifested a symmetric polyneuropathy pattern. Distribution of muscle weakness and sensory deficit was also similar between the two groups. For most patients, paresthesia and weakness were prominent in the lower limbs. In both groups most patients similarly manifested both muscle weakness and sensory deficits, while three patients in the NSVN group (13%) reported only paresthesia in the limbs without weakness. Painful sensations were reported by 74% and 65% of patients with NSVN and MPAN, respectively. None of the patients in the NSVN group but two in the MPAN group (5%) manifested facial nerve palsy. Functional impairment of patients estimated by modified Rankin scale was 2.7 ± 1.2 and 3.8 ± 0.9 ($p<0.01$) in respective groups with NSVN and MPAN. Overall, no significant difference was seen between these two groups except for functional status, although wide variation of clinical course and features were seen within each group.

3.3. Laboratory findings

Indices of extent of systemic infiltration including C-reactive protein, erythrocyte sedimentation rate, white blood

Table 2
Neurologic features of NSVN and MPAN

	NSVN (n=23)	MPAN (n=40)	p values
Neuropathic symptoms			
Initial symptom			
Paresthesia or pain	21 (91%)	34 (85%)	NS
Weakness	2 (9%)	6 (15%)	
Progression			
3 months>	10 (43%)	23 (56%)	NS
3 months<1 year	9 (39%)	13 (33%)	
1 year<	4 (17%)	4 (11%)	
Type			
Multiple mononeuropathy	18 (78%)	32 (80%)	NS
Polyneuropathy	5 (22%)	8 (20%)	
Presence of weakness			
Upper limbs	16 (70%)	30 (75%)	NS
Lower limbs	19 (83%)	40 (100%)	NS
Presence of sensory deficit			
Upper limbs	19 (83%)	25 (63%)	NS
Trunk	0 (0%)	1 (3%)	NS
Lower limbs	23 (100%)	39 (98%)	NS
Relative degree of weakness and sensory deficit			
Motor-dominant	10 (43%)	21 (53%)	NS
Sensory-dominant	10 (43%)	19 (48%)	
Pure sensory	3 (13%)	0 (0%)	
Painful sensation	17 (74%)	26 (65%)	NS
Cranial nerve involvement	0 (0%)	2 (5%)	NS
Functional status (modified Rankin score)	2.7±1.2	3.8±0.9	<0.01

NS=not significant.
Probability was determined with the Mann–Whitney U-test or the χ^2 test as appropriate.
Values are expressed as the number of patients with percentage in the parenthesis or the mean±S.D.

Table 3
Laboratory features of NSVN and MPA

	NSVN (n=23)	MPAN (n=40)	p values
Laboratory data			
CRP (mg/dl)	0.5±0.7	10.4±4.7	<0.0001
ESR (mm/h)	22±22	92±36	<0.0001
WBC (no./mm³)	5874±1818	11,738±4722	<0.0001
IgG (mg/dl)	1467±449	2035±703	<0.01
Presence of			
RF	2/17 (12%)	17/26 (65%)	<0.0001
ANA	8/22 (36%)	11/30 (37%)	NS
Anti-DNA antibody	0/17 (0%)	0/21 (0%)	NS
p-ANCA	0/21 (0%)	26/34 (76%)	<0.0001
Anti-RNP antibody	0/8 (0%)	0/12 (0%)	NS
Anti-SS-A or B antibody	0/13 (0%)	2/14 (14%)	NS
CSF protein (mg/dl)	44.1±21.9	33.6±19.9	NS

CRP=C-reactive protein; ESR=erythrocyte sedimentation rate; WBC=white blood cell; RF=rheumatoid factor; ANA=antinuclear antibody; p-ANCA=perinuclear anti-neutrophil cytoplasmic antibodies; anti-RNP antibody=anti-ribonucleoprotein antibody; CSF=cerebrospinal fluid; NS=not significant.
Probability was determined with the Mann–Whitney U-test.
Values are expressed as the number of patients with percentage in the parenthesis or the mean±S.D.

cell count, and plasma IgG level were mostly normal or only slightly abnormal in the group with NSVN, while they were mostly elevated in the group with MPAN (Table 3). Rheumatoid factor was detected in only a minority of patients in the NSVN group (12%), but was present in 65% of the MPAN group. Antinuclear antibody was detected in one-third of patients in both groups, while anti-DNA antibody was not detected in any patient in either group. Perinuclear anti-neutrophil cytoplasmic antibody (p-ANCA) was not detected in any patient in the NSVN group, but was found in 76% of patients in the MPAN group. Cerebrospinal fluid protein was 44.1±21.9 mg/dl in the NSVN group and 33.6±19.9 mg/dl in the MPAN group (no significant difference).

3.4. Electrophysiologic findings

Results of nerve conduction studies indicated axonal neuropathy in both groups (Table 4). Motor nerve conduction velocity (MCV) and distal latency (DL) were relatively preserved in both groups, while amplitude reduction of compound muscle action potentials (CMAPs) and sensory nerve action potentials (SNAPs) were conspicuous. Reduction of CMAPs and SNAPs was more predominant in the lower than the upper extremities in both groups. SNAPs in the median nerve and CMAPs in the tibial nerve showed significantly more profound reduction in MPAN than in NSVN ($p<0.01$).

Table 4
Nerve conduction studies

	NSVN (n=23)	MPAN (n=40)	p values	Controls
Median nerve				
MCV (m/s)	50.8±5.5	50.5±6.9	NS	57.8±3.7
DL (ms)	4.0±1.0	4.7±2.6	NS	3.4±0.4
CMAP (mV)	7.5±5.6	5.7±5.0	NS	10.7±3.5
Not elicited	none	2 cases (5%)		
SCV (m/s)	51.6±6.6	50.4±7.3	NS	57.8±4.7
SNAP (μV)	12.3±10.8	14.5±16.7	<0.01	23.5±8.4
Not elicited	1 case (4%)	7 cases (18%)		
Tibial nerve				
MCV (m/s)	40.2±5.3	39.5±5.2	NS	46.9±3.5
DL (ms)	4.8±2.5	5.0±0.9	NS	4.5±0.8
CMAPs (mV)	7.0±8.9	2.2±3.4	<0.01	10.9±3.8
Not elicited	3 cases (13%)	13 cases (33%)		
Sural nerve				
SCV (m/s)	45.2±9.0	41.1±10.0	NS	51.0±5.1
SNAP (μV)	3.6±8.2	1.3±3.1	NS	11.5±4.7
Not elicited	14 cases (61%)	30 cases (75%)		

MCV=motor nerve conduction velocity; DL=distal latency; CMAPs=compound muscle action potentials; SCV=sensory nerve conduction velocity; SNAPs=sensory nerve action potentials; NS=not significant.
Probability was determined with the Mann–Whitney U-test among NSVN and MPAN groups.
Values are expressed as the mean±S.D.
Control values were obtained in 191 normal volunteers for the median nerve, 121 for the tibial nerve, and 133 for the sural nerve according to the previous reports [16,19].

3.5. Pathologic findings of the sural nerves

Pathologic examination of sural nerve specimens of both NSVN and MPAN groups demonstrated profound myelinated fiber loss (Table 5). Myelinated fiber density was reduced significantly more in MPAN than in NSVN (NSVN, 2353 ± 2143 fibers/mm^2; MPAN, 1292 ± 1317 fibers/mm^2, $p < 0.05$). Both large and small myelinated fibers were reduced in both groups. In teased-fiber preparations, few fibers showed segmental demyelination and remyelination in either group ($3.0 \pm 5.5\%$ for NSVN and $1.1 \pm 2.4\%$ for MPAN). Frequency of axonal degeneration was $58.9 \pm 37.5\%$ in the NSVN group and $79.5 \pm 29.9\%$ in the MPAN group, being significantly more conspicuous in MPAN ($p < 0.05$). Vasculitis was almost completely confined to epineurial as opposed to endoneurial blood vessels in both groups. Diameters of involved arteries were 98 ± 87 μm in the NSVN group and 106 ± 91 μm in the MPAN group (no significant difference). Immunohistochemical study showed a similar profile of infiltrating cells between the two groups. Most infiltrating cells were seen surrounding vessels or within vessel walls showing vasculitis. A small proportion of CD68-positive cells, apparently macrophages, was sparsely present throughout the endoneurium. In the perivascular infiltrates, most cells were CD45-posivive, suggesting T lymphocytes. Proportions of these T lymphocytes among all infiltrating cells were $78 \pm 13\%$ in the NSVN group and $76 \pm 15\%$ in the MPAN group, while proportions of CD68-positive cells (macrophages) were $20 \pm 13\%$ and $24 \pm 15\%$ in these respective groups. CD20-positive cells, suggestive of B lymphocytes, were scant in both groups. The CD4 to CD8 ratio was similar between the two groups (1.8 ± 1.1 in NSVN, 1.5 ± 1.1 in MPAN).

Table 5
Pathology of the sural nerves

	NSVN ($n=23$)	MPAN ($n=40$)	p values	Controls ($n=9$)
Total MFD (no./mm^2)	2353 ± 2143	1292 ± 1317	<0.05	8190 ± 511
Large MFD (no./mm^2)	737 ± 872	402 ± 419	NS	3068 ± 294
Small MFD (no./mm^2)	1616 ± 1318	890 ± 981	<0.05	5122 ± 438
Teased-fiber study				
De-/remyelination (%)	3.0 ± 5.5	1.1 ± 2.4	NS	9.5 ± 8.8
Axonal degeneration (%)	58.9 ± 37.5	79.5 ± 29.9	<0.05	1.7 ± 1.4
Diameter of artery with angitis (μm)	98 ± 87	106 ± 91	NS	
Cell marker (%)				
CD45	78 ± 13	76 ± 15	NS	
CD68	20 ± 13	24 ± 15	NS	
CD20	3 ± 2	2 ± 3	NS	
CD4/CD8 ratio	1.8 ± 1.1	1.5 ± 1.1	NS	

MFD = myelinated fiber density, NS = not significant.
Probability was determined with the Mann–Whitney U-test among NSVN and MPAN groups.
Values are expressed as the mean ± S.D.
Control values are based on previously published reports [14,18].

4. Discussion

Although NSVN is clinically distinctive from other systemic vasculitides such as MPA in that clinically apparent vasculitis is confined to the peripheral nervous system, uncertainty prevails as to whether NSVN is likely to have a distinct etiology and pathogenesis and to represent an independent disease entity. The nosologic relationship between NSVN and MPA-associated neuropathy (MPAN) therefore remains in question. Although MPA frequently involves lung and kidney, the Chapel Hill consensus conference criteria do not limit MPA to cases with renal or pulmonary manifestations; the definition is based instead solely on the presence of small-vessel involvement [7]. Considering reports of vasculitis confined to a single organ such as the skin [20], gastrointestinal viscera [21], uterine cervix [22], urinary bladder [23], lungs [24], kidneys [25], or central nervous system [26], features of MPA might differ artifactually between series of patients collected by different medical specialists [5]. As for NSVN, a reported patient initially given this diagnosis showed systemic manifestations 12 years later [27]. Patients with pathologically proven vasculitis in both skin and peripheral nerve but manifesting no other systemic symptoms have also been reported [28,29]. Even p-ANCA-positive vasculitis confined to peripheral nerves without systemic symptoms has been reported [30]. Furthermore, a significant proportion of vasculitic neuropathy patients with vasculitis clinically confined to peripheral nerves nonetheless showed vasculitis in muscle specimens [9,31]. Thus, patients with vasculitis in the peripheral nervous system might harbor concomitant asymptomatic vasculitis in other organs such as liver, lung, or muscle, but still be likely to be diagnosed with NSVN. If nonneural involvement develops, the patient is likely to be diagnosed with MPA. Because the definition of these vasculitic neuropathies remains a little vague, some overlap may present.

One striking clinical difference reported between NSVN and systemic vasculitis with peripheral nerve involvement, such as MPAN, is the reported prognosis [32]. MPA tends to involve the kidney or lung, whose function is essential for life, so patients with renal or pulmonary involvement show a relatively unfavorable prognosis [5]. However, MPA without involvement of the kidney or lung has been found to carry a good prognosis similar to that of NSVN [5]. Although NSVN has been considered to show a relatively good prognosis, a previous study reported that combination therapy including a steroid and a cytotoxic agent (usually cyclophosphamide) had a more favorable effect on prognosis than steroid monotherapy [33]. Such superior efficacy of combination therapy in NSVN parallels findings in other systemic vasculitides including MPA [34]. These observations also support the view that etiologies of NSVN and MPA may overlap, and these disorders may share common pathogenic mechanism to some extent.

In this study we compared clinicopathologic features of NSVN and MPAN. Clinical, electrophysiologic, and histo-

pathologic features showed similarity to some extent between the two groups but the age at onset, severity, and presence of p-ANCA were clearly different. Neuropathic symptoms were similar in terms of initial symptom, progression, and distribution and relative degree of muscle weakness and sensory deficits but severity as determined by the modified Rankin score was more profound in MPAN. Electrophysiologic and histopathologic findings indicated axonal neuropathy in both groups but SNAPs of the median nerve, CMAPs of the tibial nerve, myelinated fiber density, and degree of axonal degeneration showed more severe involvement in MPAN than NSVN, reflecting overall greater clinical severity. As for the nature of the vasculitic lesion, a previous study reported that NSVN was characterised by involvement of small vessels less than 40 μm in diameter [35]. In our comparative study of sural nerve biopsy specimens, mean size of the involved epineurial vessels did not differ significantly between MPAN and NSVN. Laboratory data, particularly for indicators of the extent of systemic inflammation or the likelihood of collagen diseases, were clearly different between the two groups. These differences may reflect severity of the systemic inflammatory process or severity of other organ involvement rather than the nature of inflammatory profile in the two groups. Patterns of cell marker profiles among infiltrating cells were also similar in both groups.

Similar clinicopathologic profiles and vascular pathology suggest that NSVN may be a part of a continuum in the spectrum of systemic necrotizing and inflammatory vascular diseases such as MPA, but some differences may still suggest that NSVN is distinct from systemic vasculitides. Further study is needed to clarify the pathogenesis of NSVN and its place in the vasculitic spectrum of diseases.

References

[1] Rosenbaum R. Neuromuscular complications of connective tissue diseases. Muscle Nerve 2001;24:154–69.

[2] Kernohan JW, Woltman HW. Periarteritis nodosa: clinicopathologic study with special reference to the nervous system. Arch Neurol Psychol 1938;39:655–86.

[3] Kissel JT, Slivka AP, Warmolts JR, Mendell JR. The clinical spectrum of necrotizing angiopathy of the peripheral nervous system. Ann Neurol 1985;18:251–7.

[4] Dyck PJ, Benstead TJ, Conn DL, Stevens JC, Windebank AJ, Low PA. Nonsystemic vasculitic neuropathy. Brain 1987;110:843–53.

[5] Guillevin L, Durand-Gasselin B, Cevallos R, Gayraud M, Lhote F, Callard P, et al. Microscopic polyangiitis: clinical and laboratory findings in eighty-five patients. Arthritis Rheum 1999;42:421–30.

[6] Davson J, Ball J, Platt R. The kidney in periarteritis nodosa. Q J Med 1948;17:175–202.

[7] Jennette JC, Falk RJ, Andrassy K, Bacon PA, Churg J, Gross WL, et al. Nomenclature of systemic vasculitides. Proposal of an international consensus conference. Arthritis Rheum 1994;37:187–92.

[8] Guillevin L, Lhote F, Amouroux J, Gherardi R, Callard P, Casassus P. Antineutrophil cytoplasmic antibodies, abnormal angiograms and pathological findings in polyarteritis nodosa and Churg-Strauss syndrome: indications for the classification of vasculitides of the polyarteritis Nodosa Group. Br J Rheumatol 1996;35:958–64.

[9] Collins MP, Mendell JR, Periquet MI, Sahenk Z, Amato AA, Gronseth GS, et al. Superficial peroneal nerve/peroneus brevis muscle biopsy in vasculitic neuropathy. Neurology 2000;55:636–43.

[10] van Swieten JC, Koudstaal PJ, Visser MC, Schouten HJ, van Gijn J. Interobserver agreement for the assessment of handicap in stroke patients. Stroke 1988;19:604–7.

[11] Kimura J. Principles of nerve conduction studies. In: Kimura J, editor. Electrodiagnosis in diseases of nerve and muscle: principles and practice, 2nd ed. Philadelphia: F.A. Davis, 1989. p. 78–102.

[12] Kimura J. Assessment of individual nerves. In: Kimura J, editor. Electrodiagnosis in diseases of nerve and muscle: principles and practice, 2nd ed. Philadelphia: F.A. Davis, 1989. p. 103–38.

[13] Sobue G, Yasuda T, Mitsuma T, Ross AH, Pleasure D. Expression of nerve growth factor receptor in human peripheral neuropathies. Ann Neurol 1988;24:64–72.

[14] Sobue G, Hashizume Y, Mukai E, Hirayama M, Mitsuma T, Takahashi A. X-linked recessive bulbospinal neuronopathy. A clinicopathological study. Brain 1989;112:209–32.

[15] Hattori N, Ichimura M, Nagamatsu M, Li M, Yamamoto K, Kumazawa K, et al. Clinicopathological features of Churg-Strauss syndrome-associated neuropathy. Brain 1999;122:427–39.

[16] Koike H, Iijima M, Sugiura M, Mori K, Hattori N, Ito H, et al. Alcoholic neuropathy is clinicopathologically distinct from thiamine-deficiency neuropathy. Ann Neurol 2003;54:19–29.

[17] Dyck PJ, Giannini C, Lais A. Pathologic alterations of nerves. In: Dyck PJ, Thomas PK, Griffin JW, et al, editors. Peripheral neuropathy, 3rd ed. Philadelphia: W. B. Saunders, 1993. p. 514–95.

[18] Nagamatsu M, Terao S, Misu K, Li M, Hattori N, Ichimura M, et al. Axonal and perikaryal involvement in chronic inflammatory demyelinating polyneuropathy. J Neurol Neurosurg Psychiatry 1999;66: 727–33.

[19] Koike H, Mori K, Misu K, Hattori N, Ito H, Hirayama M, et al. Painful alcoholic polyneuropathy with predominant small-fiber loss and normal thiamine status. Neurology 2001;56:1727–32.

[20] Daoud MS, Hutton KP, Gibson LE. Cutaneous periarteritis nodosa: a clinicopathological study of 79 cases. Br J Dermatol 1997;136: 706–13.

[21] Burke AP, Sobin LH, Virmani R. Localized vasculitis of the gastrointestinal tract. Am J Surg Pathol 1995;19:338–49.

[22] Woywodt A, Schneider W, Morack G, Kettritz R, Goebel U. Necrotizing small-vessel vasculitis confined to the uterine cervix. Semin Arthritis Rheum 2000;29:368–72 [Review].

[23] Fischer AH, Wallace VL, Keane TE, Clarke HS. Two cases of vasculitis of the urinary bladder: diagnostic and pathogenetic considerations. Arch Pathol Lab Med 1998;122:903–6.

[24] Jennings CA, King Jr TE, Tuder R, Cherniack RM, Schwarz MI. Diffuse alveolar hemorrhage with underlying isolated, pauciimmune pulmonary capillaritis. Am J Respir Crit Care Med 1997;155: 1101–9.

[25] Medvedev G, Al-Shamari AE, Copland MA, Magil AB. Isolated renal giant cell arteritis. Am J Kidney Dis 2002;40:658–61.

[26] Calabrese LH, Furlan AJ, Gragg LA, Ropos TJ. Primary angiitis of the central nervous system: diagnostic criteria and clinical approach. Cleve Clin J Med 1992;59:293–306.

[27] Greenberg SA. P-ANCA vasculitic neuropathy with 12-year latency between onset of neuropathy and systemic symptoms. BMC Neurol 2002;2:10.

[28] Satoh J, Yamamoto T, Kuroda Y. Vasculitis confined to the peripheral nerve and skin: a variant of non-systemic vasculitic neuropathy. Eur J Neurol 1999;6:241–4.

[29] Hagiwara N, Sekijima Y, Hattori T, Hashimoto T, Ikeda S. Two patients with different types of vasculitic neuropathy: a comparison between cutaneous polyarteritis nodosa and nonsystemic vasculitic neuropathy. Rinsho Shinkeigaku 2003;43:102–8.

[30] Oguni E, Watanabe S, Nagata H, Mizusawa H, Shoji S. A case of nonsystemic vasculitic neuropathy with anti-neutrophil cytoplasm antibody (ANCA). Rinsho Shinkeigaku 1994;34:470–3.

[31] Said G, Lacroix-Ciaudo C, Fujimura H, Blas C, Faux N. The peripheral neuropathy of necrotizing arteritis: a clinicopathological study. Ann Neurol 1988;23:461–5.

[32] Davies L, Spies JM, Pollard JD, McLeod JG. Vasculitis confined to peripheral nerves. Brain 1996;119:1441–8.

[33] Collins MP, Periquet MI, Mendell JR, Sahenk Z, Nagaraja HN, Kissel JT. Nonsystemic vasculitic neuropathy: insights from a clinical cohort. Neurology 2003;61:623–30.

[34] Gayraud M, Guillevin L, le Toumelin P, Cohen P, Lhote F, Casassus P, et al. Long-term follow up of polyarteritis nodosa, microscopic polyangiitis, and Churg-Strauss syndrome: analysis of four prospective trial including 278 patients. Arthritis Rheum 2001;44:666–75.

[35] Ohkoshi N, Mizusawa H, Oguni E, Shoji S. Sural nerve biopsy in vasculitic neuropathies: morphometric analysis of the caliber of involved vessels. J Med 1996;27:153–70.

Archaeal Proteasomes Effectively Degrade Aggregation-prone Proteins and Reduce Cellular Toxicities in Mammalian Cells[*]

Shin-ichi Yamada, Jun-ichi Niwa, Shinsuke Ishigaki, Miho Takahashi, Takashi Ito, Jun Sone, Manabu Doyu, and Gen Sobue[1]

From the Department of Neurology, Nagoya University Graduate School of Medicine, 65 Tsurumai-cho, Showa-ku, Nagoya-city, Aichi 466-8550, Japan

The 20 S proteasome is a ubiquitous, barrel-shaped protease complex responsible for most of cellular proteolysis, and its reduced activity is thought to be associated with accumulations of aberrant or misfolded proteins, resulting in a number of neurodegenerative diseases, including amyotrophic lateral sclerosis, spinal and bulbar muscular atrophy, Parkinson disease, and Alzheimer disease. The 20 S proteasomes of archaebacteria (archaea) are structurally simple and proteolytically powerful and thought to be an evolutionary precursor to eukaryotic proteasomes. We successfully reproduced the archaeal proteasome in a functional state in mammalian cells, and here we show that the archaeal proteasome effectively accelerated species-specific degradation of mutant superoxide dismutase-1 and the mutant polyglutamine tract-extended androgen receptor, causative proteins of familial amyotrophic lateral sclerosis and spinal and bulbar muscular atrophy, respectively, and reduced the cellular toxicities of these mutant proteins. Further, we demonstrate that archaeal proteasome can also degrade other neurodegenerative disease-associated proteins such as α-synuclein and tau. Our study showed that archaeal proteasomes can degrade aggregation-prone proteins whose toxic gain of function causes neurodegradation and reduce protein cellular toxicity.

The 20 S proteasome is a ubiquitous, barrel-shaped protease complex responsible for most of cellular proteolysis (1) and is formed by four stacked seven-membered rings (2). The α-type subunits, which are proteolytically inactive (3), form the outer rings, and the β-type subunits, which contain the active site (4), form the inner rings of the complex (5). The 20 S proteasome of archaebacteria (archaea) consists of only one type of each of the α- and β-subunits and is thought to be the evolutionary ancestor of the eukaryotic proteasome (6), which is quite similar in architecture to that of archaea but is composed of seven different α- and seven different β-subunits (6). Archaea do not have the ubiquitin recognition system for protein degradation and

are thought to have unidentified tags in its degradation pathway (7). Like eukaryotic cells, archaea also have a regulatory complex for the 20 S proteasome, known as proteasome-activating nucleotidase (PAN)[2] (8). PAN is an evolutionary precursor to the 19 S base in eukaryotic cells and thought to be necessary for efficient archaeal 20 S proteasomal protein degradation (8). However *in vitro*, the archaeal 20 S proteasome has been reported to rapidly degrade polyglutamine aggregates without the help of PAN (9). This PAN-independent degradation by the archaeal 20 S proteasome inspired us to introduce and test a novel proteolytic facility in mammalian cells. We have chosen the archaeal *Methanosarcina mazei* (Mm) 20 S proteasome, because its optimal growth temperature is around 37 °C, making it suitable to examine its proteasomal effects in mammalian cells.

The eukaryotic ubiquitin-proteasome system degrades aberrant or misfolded proteins that could otherwise form potentially toxic aggregates (10). These aggregate formations in cells are related to the pathogenesis of several common aging-related neurodegenerative diseases, including Parkinson disease (PD), amyotrophic lateral sclerosis (ALS), polyglutamine diseases (e.g. Huntington disease, some spinocerebellar ataxias, and spinal and bulbar muscular atrophy), and Alzheimer disease (AD), which are thought to be associated with the reduced activities of the proteasome (11–15). However, a critical cause of the accumulation of abnormal proteins remains unclear. Solving this common aspect of many neurodegenerative disorders would be a breakthrough in treating these diseases.

In the present study, we show that the Mm proteasome functions in mammalian cells to accelerate the degradation of the following aggregation-prone proteins: mutant superoxide dismutase-1 (SOD1), a causative protein of familial ALS; mutant androgen receptor (AR) with expanded polyglutamine tract, a causative protein of spinal and bulbar muscular atrophy; α-synuclein, an accumulated protein in PD; and tau, an accumulated protein in AD.

[2] The abbreviations used are: PAN, proteasome-activating nucleotidase; SOD1, superoxide dismutase-1; Mm, *M. mazei*; ALS, amyotrophic lateral sclerosis; AR, androgen receptor; PD, Parkinson disease; AD, Alzheimer disease; MTS, 3-(4,5-dimethylthiazol-2-yl)-5-(3-carboxymethoxyphenyl)-2-(4-sulfophenyl)-2H-tetrazolium; WT, wild type; NTA, nitrilotriacetic acid; GFP, green fluorescent protein.
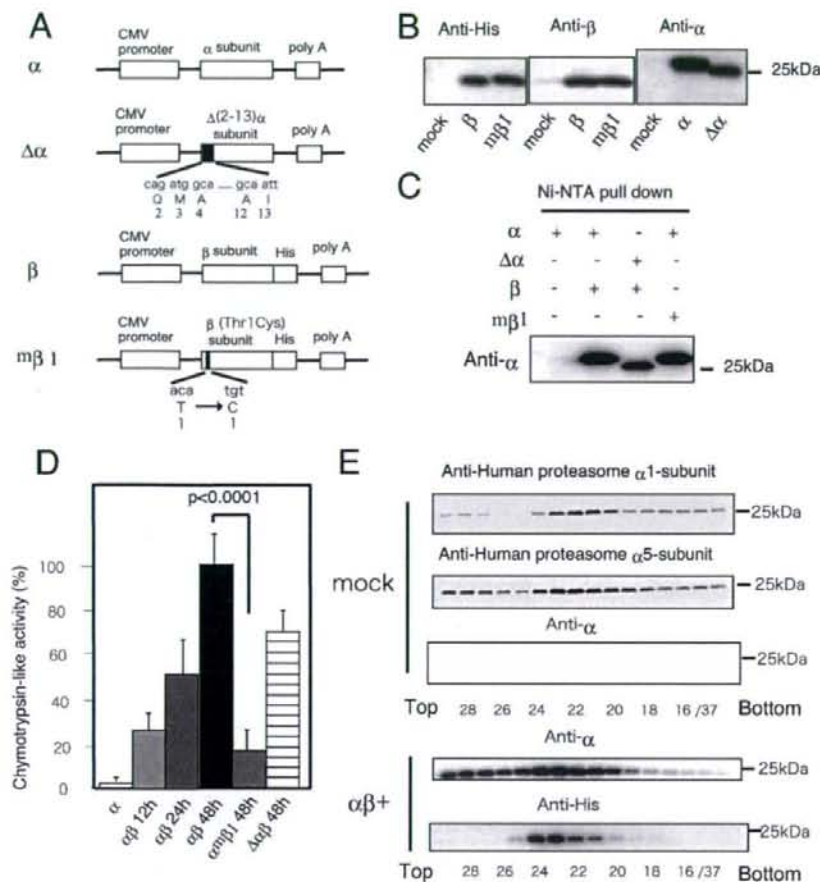
FIGURE 1. **Expression of *M. mazei* proteasome in mammalian cells.** *A*, schematic illustration of expression vectors used in this study. The deleted sequences of the Δα-subunit are depicted. The T1C β-subunit (mβ1) has three mutated base pairs (a to t, c to g, and a to t). *B*, Western blot analysis with anti-proteasome α-subunit, anti-proteasome β-subunit, and anti-His antibodies. *C*, Ni²⁺-NTA pulldown assay. Pulled down proteins run on SDS-PAGE were probed with anti-proteasome α-subunit. *D*, chymotrypsin-like activity of the Ni²⁺-NTA pulled down samples. This protease activity gradually became higher after transfection. *Error bars*, S.D. (*n* = 3). *E*, glycerol gradient centrifugation experiment: Mm proteasome α- and β-subunits fractionated into nearly the same fractions as did the human 20 S proteasome subunits α1 and α5, αβ− and αβ+, indicating that cells were transfected with mock and Mm proteasome αβ, respectively.

CTG) and inserted into the XbaI and AgeI site of the pcDNA3.1(+)/MycHis vector (Invitrogen) to fuse it to a His₆ tag. The mutated mβ1-subunit (T1C β-subunit) was generated with a site-directed mutagenesis kit (Stratagene) following the manufacturer's protocol. Construction of pcDNA3.1/MycHis-SOD1 and pCMV-Tag4-SOD1 vectors (WT, G93A, G85R, H46R, and G37R) (16), pEGFP-N1-SOD1 (WT and G93A) vectors, pCR3.1-AR24Q and pCR3.1-AR97Q vectors, and pcDNA3.1(+)/MycHis-α-synuclein (WT, A53T, and A30P) was described previously (16–18). Six isoforms of tau were amplified by PCR from the pRK172 vectors that were kindly provided by Dr. Michel Goedert and inserted into the KpnI and XbaI site of the pcDNA3.1 vector (Invitrogen).

Cell Culture, Transfection, and Antibodies—Neuro2a cells and human embryonic kidney 293 (HEK293) cells were maintained in Dulbecco's modified Eagle's medium with 10% fetal calf serum. Transfections were performed using Lipofectamine 2000 (Invitrogen) in the 3-(4,5-dimethylthiazol-2-yl)-5-(3-carboxymethoxyphenyl)-2-(4-sulfophenyl)-2H-tetrazolium (MTS) assay or Effectene transfection reagent (Qiagen) in other experiments. Antibodies used here were as follows: anti-SOD1 antibody (SOD100; Stressgen Bioreagents), anti-His antibody (Ab-1; Oncogene), anti-α-tubulin antibody (clone B-5-1-1; Sigma), anti-20 S proteasome β-subunit antibody (from *Methanosarcina thermophila*; Calbiochem), anti-20 S proteasome α-subunit antibody (from *M. thermophila*; Calbiochem), anti-AR antibody (N-20; Santa Cruz Biotechnology, Inc., Santa Cruz, CA), anti-α-synuclein antibody (LB509; Zymed Laboratories Inc.), and anti-tau antibody (Mouse Tau-1; Chemicon International).

EXPERIMENTAL PROCEDURES

Construction of the Expression Vectors: M. mazei Proteasome Subunits α, β, ΔN(2–13)α, and Mutant β (T1C)—The DNA fragment encoding the α-subunit protein (GenBank™ accession number 1480962) was amplified by PCR from the genomic DNA of *M. mazei* (ATCC) using the following primers: αF (5′-GCGGGTACCCCACCATGCAGATGGCACCACAGATG) and αR (5′-CGCCTCGAGTTATTCTTTGTTCTCATTTCCTTTGTG). The Δ(2–13) α-subunit (Δα) was amplified using the following primers: ΔαF (5′-GCGGGTACCCCACCATGACGGTTTTCAGCCCTGACGG) and αR. The amplified fragments were inserted into the KpnI and XhoI site of the pcDNA 3.1(+) vector (Invitrogen). The β-subunit (GenBank™ accession number 1479036) was amplified by PCR with the following primers: βF (5′-GCCTCTAGACCACCATGGATAATGACAAATATTTAAAG) and βR (5′-GCGACCGGTGTTTCCTAAAGCTCTT-

Glycerol Density Gradient Centrifugation—Cells grown on a 10-cm dish were lysed in 1 ml of 0.01 M Tris-EDTA, pH 7.5, by two freeze-thaw cycles, and the lysates were centrifuged for 15 min at 15 000 × *g* at 4 °C. The cleared supernatants were loaded on the top of a 36-ml linear gradient of glycerol (10–40%) prepared in 25 mM Tris-HCl buffer, pH 7.5, containing 1 mM dithiothreitol and then centrifuged at 80,000 × *g* for 22 h at 4 °C in a Beckman SW28 rotor (Beckman Coulter Inc.). Following centrifugation, 37 fractions (1.0 ml each) were collected from the top of the tubes with a liquid layer injector fractionator (model number CHD255AA; Advantech) connected to a fraction col-
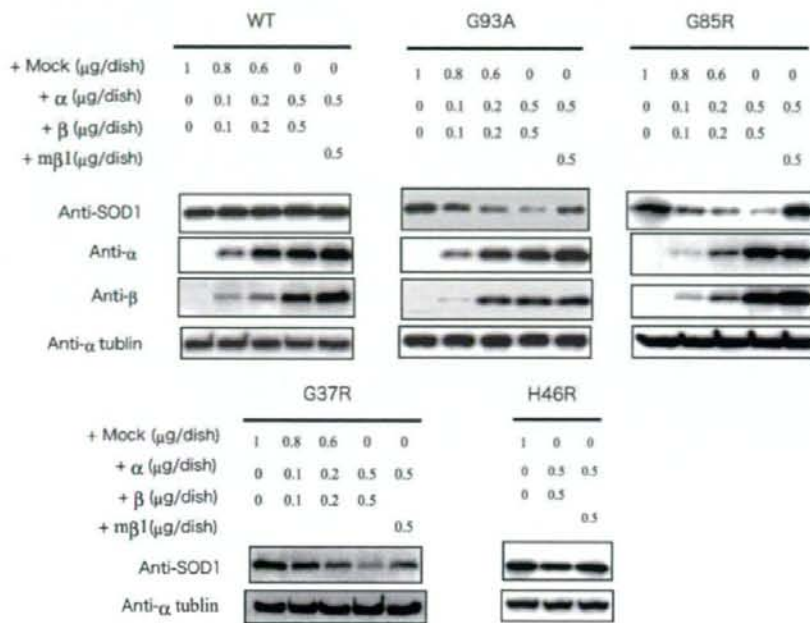
- 232 -

FIGURE 2. Reduced expression levels of mutant SOD1 proteins in the presence of *M. mazei* proteasome. Neuro2a cells grown on 6-cm dishes and co-transfected with 1 μg of SOD1-MycHis vector and increasing doses of Mm proteasome subunits were harvested and analyzed 48 h after transfection. The levels of mutant SOD1 proteins were gradually reduced as Mm proteasome $\alpha\beta$ increased, whereas no changes in SOD1 proteins were seen with Mm proteasome αmβ1. *WT*, wild-type SOD1; *G93A*, SOD1^{G93A}; *G85R*, SOD1^{G85R}; *G37R*, SOD1^{G37R}; *H46R*, SOD1^{H46R}.

lector. 200 μl of each fraction was precipitated with acetone; the pellets were lysed with 50 μl of sample buffer and then used for SDS-PAGE followed by Western blotting. The immunostained bands were quantified using ImageGauge software (Fuji Film).

Ni^{2+}-NTA Pulldown—HEK 293 cells grown on 10-cm dishes, transfected with Mm proteasome α (as a control), $\alpha\beta$, $\Delta\alpha\beta$, and αmβ1, were lysed by two freeze-thaw cycles in 1 ml of phosphate-buffered saline buffer and centrifuged at 3000 $\times$ *g*. Proteasome complexes were pulled down from the supernatants with 200 μl of Ni^{2+}-NTA-agarose, washed 4 times in 4 ml of 10 m$_M$ imidazole/phosphate-buffered saline buffer, and eluted in 2 ml of 250 m$_M$ imidazole/phosphate-buffered saline buffer. Samples were then boiled and subjected to Western blotting.

Measurement of the Proteasome Activity—HEK 293 cells grown on 10-cm dishes were transfected with Mm proteasome α (as a control), $\alpha\beta$, $\Delta\alpha\beta$, and αmβ1. 12, 24, and 48 h after transfection, the cells were lysed and pulled down with Ni^{2+}-NTA. The chymotrypsin-like activity of 500 μl of the Ni^{2+}-NTA pulled down samples were assayed colorimetrically after 12-h incubations at 37 °C with 100 m$_M$ Suc-LLVY-amino-4-methylcoumarin (Sigma) by a multiple-plate reader (PowerscanHT, Dainippon Pharmaceutical). The assay was carried out in triplicate and statistically analyzed by one-way analysis of variance.

Immunocytochemistry—Neuro2a cells grown on glass coverslips were co-transfected with pEGFP-N1-SOD1 and Mm proteasome α- and His-tagged β-subunit. 48 h after transfection, cells were fixed, blocked, and incubated with anti-His antibody

overnight at 4 °C. After washing, samples were incubated with Alexa-546-conjugated anti-mouse antibody (Molecular Probes, Inc.) and visualized with an Olympus BX51 epifluorescence microscope.

Cycloheximide Chase Analysis—Neuro2a cells grown on 6-cm dishes were transfected with 1 μg of pcDNA3.1/MycHis-SOD1 with mock (0.6 μg), Mm proteasome αmβ1 (0.3 μg each), or Mm proteasome $\alpha\beta$ (0.3 μg each). 24 h after transfection, cycloheximide (50 μg/ml) was added to the culture medium, and the cells were harvested at the indicated time points. The samples were subjected to SDS-PAGE and analyzed by Western blotting with anti-SOD1 antibody.

Pulse-chase Analysis—Neuro2a cells grown on 6-cm dishes were transfected with 1 μg of pCMV-Tag4-SOD1^{G93A} with mock (0.6 μg) Mm proteasome αmβ1 (0.3 μg each) or Mm proteasome $\alpha\beta$ (0.3 μg each). 24 h after transfection, cells were pulse-labeled with [^{35}S]Cys for 60 min and harvested at the indicated time points. After the immunoprecipitation by anti-FLAG antibody (M2; Sigma), the samples were subjected to SDS-PAGE, phosphor-imaged (Typhoon 9410; Genaral Electric Co.), and statistically analyzed by one-way analysis of variance.

Cell Viability Analysis—HEK293 cells were grown on collagen-coated 96-well plates and co-transfected with pcDNA3.1/MycHis-SOD1 (WT, G93A, and G85R) and Mm 20 S proteasome $\alpha\beta$, αmβ1, or mock in 12 wells each. The MTS-based cell proliferation assays were performed after 48 h of transfection. Absorbance at 490 nm was measured at 37 °C in a multiple-plate reader (PowerscanHT, Dainippon Pharmaceutical). The assay was carried out in triplicate and statistically analyzed by one-way analysis of variance.

Caspase-3/7 Assay—HEK293 cells were grown on black 96-well plates and co-transfected with pcDNA3.1/MycHis-SOD1 (WT, G93A, and G85R) and Mm 20 S proteasome $\alpha\beta$, αmβ1, or mock. 24 h after transfection, the medium was replaced with serum-free medium (Dulbecco's modified Eagle's medium). After 24 h, activated caspase-3/7 activity was analyzed by the Apo-ONE homogeneous caspase-3/7 assay (Promega) following the manufacturer's instructions.

RESULTS

Cloning and Expression of M. mazei Proteasome—We cloned the Mm proteasome α-subunit (GenBank^{TM} accession number 1480962) and β-subunit (GenBank^{TM} accession number 1479036) from genomic DNA of Mm (Fig. 1A) and generated a mutant α-subunit lacking amino acids 2–13, Δ(2–13) α-subunit ($\Delta\alpha$) (Fig. 1A). These amino acids (positions 2–13) nor-
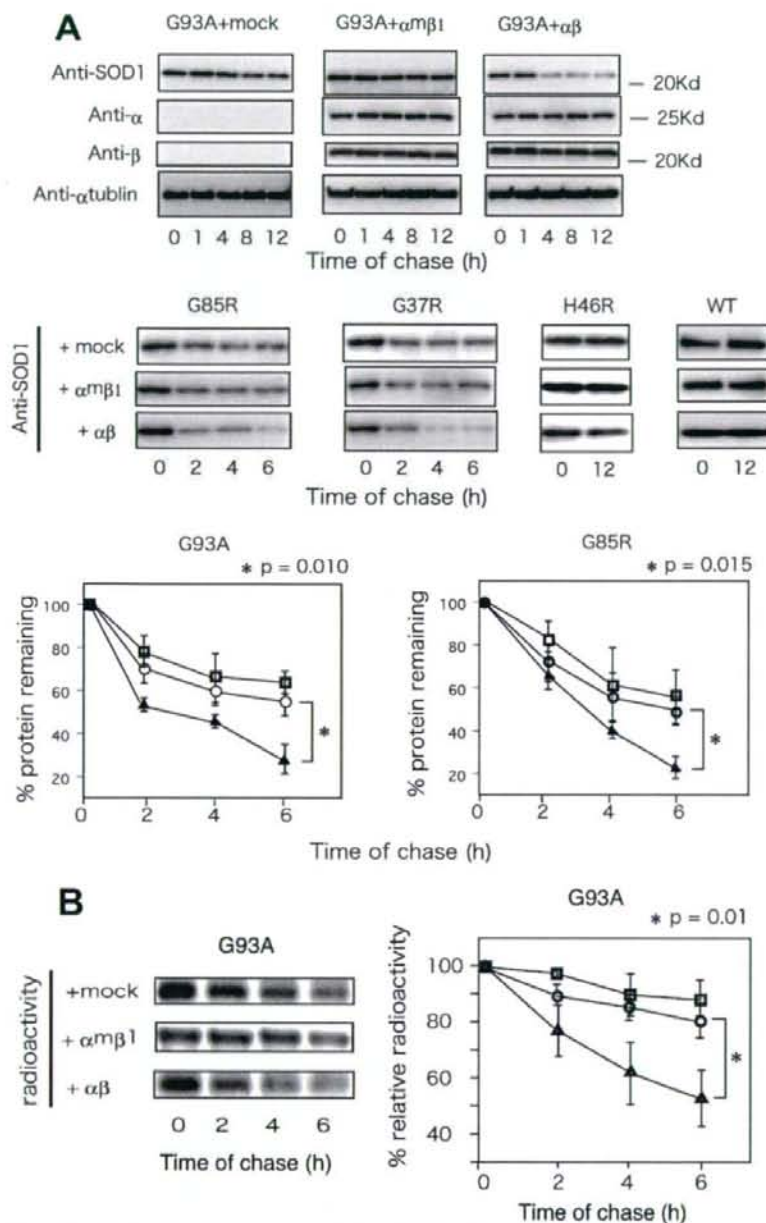
- 233 -

FIGURE 3. *M. mazei* proteasome-accelerated degradation of mutant SOD1 proteins. *A,* cycloheximide chase analysis (see "Experimental Procedures") showing that the half-lives of various mutant SOD1 proteins were reduced in the presence of Mm 20 S proteasome αβ. The *graphs* represent the percentage of degraded SOD1[G93A] and SOD1[G85R] proteins in three independent experiments. The *error bars* indicate S.D. *B,* pulse-chase analysis (see "Experimental Procedures") showing that the degradation of SOD1[G93A] was accelerated in the presence of Mm 20 S proteasome αβ. *Circle,* mock; *triangle,* αβ; *square,* αmβ1. Error bars, S.D. (*n* = 3).

following experiments were performed in both HEK293 and Neuro2a cells with similar results in both cell lines.

To confirm protein expression of the Mm subunits, HEK293 cells transfected with mock, α, Δα, β, or mβ1 were lysed, subjected to SDS-PAGE, and immunoblotted with anti-proteasome α-subunit, anti-proteasome β-subunit, and anti-His antibodies. Fig. 1*B* demonstrates that the α- and β-subunit antibodies detected the Mm proteasome α-subunit at 26 kDa, the Δα-subunit around 25 kDa, and the β-subunit at 22 kDa, respectively, and faintly recognized endogenous human proteasome subunits. A Ni^{2+}-NTA pull-down assay showed that the Mm proteasome α- and Δα-subunits co-sedimented with the Mm proteasome β- and mβ1-subunits but not with mock (Fig. 1*C*), and protease activity of the pulled down samples of the cells lysed 48 h after transfection showed significantly higher chymotrypsin-like protease activity in the Mm proteasome αβ than in the αmβ1 or mock-transfected samples (Fig. 1*D*). This protease activity was confirmed to become gradually higher after transfection (Fig. 1*D*).

Glycerol density gradient centrifugation fractionated the αβ, Δαβ, and αmβ1 complexes of the Mm proteasome into nearly the same fractions as those of the human 20 S proteasome subunits α1 and α5 (Fig. 1*E*, data not shown for Δαβ and αmβ1). Moreover, of the anti-His-immunoblotted bands (Fig. 1*E*), the density of staining in fractions 20–25 accounts for about 80–90% of the total anti-His staining. That these fractions constitute the majority of the anti-α staining as well suggests that about 80–90% of the β-subunit expression is incorporated into the Mm proteasome. These results suggested that the Mm proteasome α-, Δα-, β-, and

mally form a gated channel in the α-ring that regulates substrate entry into the 20 S proteasome (19). We also generated a mutant β-subunit with T1C (mβ1) (Fig. 1*A*). Thr-1 in the β-subunit of the archaeal proteasome is essential for proteolysis, and Thr-1 mutants lose their proteolytic activities (20). The

mβ1-subunits could properly assemble to form four stacked seven-membered rings and that an active Mm proteasome could be reproduced in mammalian cells. The cells expressing Mm proteasome Δαβ displayed cellular toxicity, whereas the cells expressing Mm proteasome αβ showed little toxicity
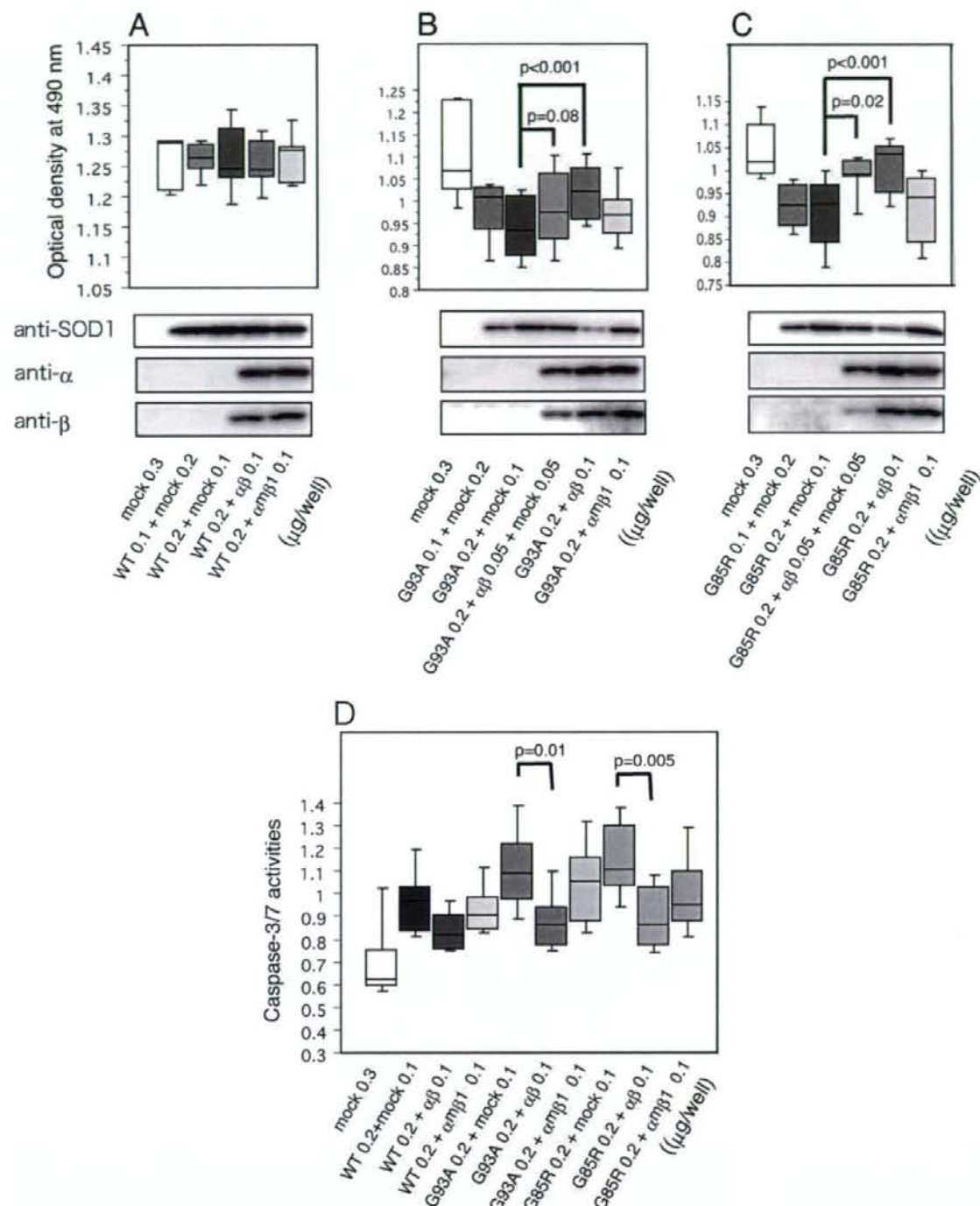
- 234 -

FIGURE 4. **M. mazei proteasome reduces the cellular toxicity of mutant SOD1.** The dose-dependent rescue effect of Mm proteasome $\alpha\beta$ expression on cell viability in SOD1^{WT}- (A), SOD1^{G93A}- (B), and SOD1^{G85R}-transfected HEK293 cells (C) as shown in MTS-based cell proliferation assays. The *box plots* show the median values (*center line* of box), the 25th (*lower line* of box), 75th (*upper line* of box), 10th (*lower T bar*), and 90th (*upper T bar*) percentiles in each group ($n = 3 \times 6$ wells). The *numbers* indicate the dose of DNA transfected in each well of a 96-well plate ($\alpha\beta$, 0.1 μg; α, 0.05 μg; β, 0.05 μg). The expression levels of SOD1, α-subunit, and β-subunit at the analyzed points are shown. D, relative activities of cleaved caspase-3/7 were analyzed with the fluorescent caspase substrate, benzyloxycarbonyl-DEVD-R110. Production of Mm proteasome $\alpha\beta$ prevents activation of caspase-3/7. Positive control value was 3.2 ± 0.2 (S.D.) ($n = 3 \times 4$ wells) (1 μM staurosporin, 24 h).

- 235 -

(data not shown); thus, further experiments were carried out with Mm proteasomes $\alpha\beta$ and $\alpha m\beta 1$.

M. mazei Proteasome Degrades Specifically Mutant Superoxide Dismutase-1—We then assessed whether the Mm proteasome actually affects mutant SOD1 protein (SOD1^{G85R}, SOD1^{G37R}, SOD1^{G93A}, and SOD1^{H46R}) expression. In cultured cells, mutant SOD1^{G85R}, SOD1^{G37R}, and SOD1^{G93A} are more likely to form aggregates than is SOD1^{H46R} (16), and cases of familial ALS expressing these mutant forms are also more severe than those expressing SOD1^{H46R}. Western blot analyses demonstrated that the levels of mutant SOD1 were markedly reduced as the expression of Mm proteasome $\alpha\beta$ increased (Fig. 2). However, wild-type SOD1 levels were not affected by the expression of Mm proteasome $\alpha\beta$. Furthermore, mutant SOD1 levels were not affected by the expression of Mm proteasome containing the mβ1-subunit in all mutant species, indicating that Mm proteasomal activity was important to reduce the levels of mutant SOD1 proteins. That the expression level of SOD1^{H46R} was less affected by Mm proteasomal expression than other mutant SOD1 species may be associated with the lower toxicity of SOD1^{H46R}.

To determine whether the reduced levels of mutant SOD1 protein were due to accelerated degradation of mutant SOD1 or to the reduction of mutant SOD1 expression, we examined the stability of mutant SOD1 proteins expressed in Neuro2a cells co-expressed with Mm proteasome $\alpha\beta$, $\alpha m\beta 1$, or mock (Fig. 3, *A* and *B*). Chase experiments with cycloheximide, which halts all cellular protein synthesis, demonstrated mutant species-dependent acceleration in SOD1 protein degradation, whereas the expression levels of Mm proteasome α- and β-subunits did not change (Fig. 3*A*). The degree of wild-type SOD1 degradation was not affected by the expression of Mm proteasome $\alpha\beta$. Pulse-chase experiments further confirmed that ^{35}S-labeled SOD1^{G93A} degradation was significantly accelerated when co-expressed with Mm proteasome $\alpha\beta$ but not with Mm proteasome $\alpha m\beta 1$ or mock (Fig. 3*B*). These facts strongly suggest that the catalytic center in the Mm proteasome β-subunit is important to accelerate the degradation of mutant SOD1 proteins.

M. mazei Proteasome Reduces Cellular Toxicities of Mutant Superoxide Dismutase-1—Next, we investigated the viability of HEK293 cells evoked by SOD1 (wild-type, SOD1^{G93A}, and SOD1^{G85R}) when co-expressed with Mm proteasome $\alpha\beta$, $\alpha m\beta 1$, or mock by the MTS-based cell proliferation assay (Fig. 4). We confirmed a linear response between cell number and optical density at 490 nm between 0.85 and 1.30 (data not shown). The viability of cells expressing wild-type SOD1 with Mm proteasome $\alpha\beta$ did not change as the transfected DNA doses of SOD1 and Mm proteasome $\alpha\beta$ increased (Fig. 4*A*). However, the viability of cells expressing mutant SOD1 was reduced as the transfected DNA dose of SOD1 increased (Fig. 4, *B* and *C*), and this reduction was prevented by the co-transfection with Mm proteasome $\alpha\beta$ but not with Mm proteasome $\alpha m\beta 1$. Toxicities of mutant SOD1 proteins are associated with the activation of caspase family proteins, especially caspase-3 (21). Using fluorescent substrates of activated caspase-3/7 as markers, we analyzed caspase-3/7 activities in the cells co-transfected with SOD1 proteins and with mock, Mm proteasome $\alpha\beta$, and $\alpha m\beta 1$. Mm proteasome $\alpha\beta$ suppressed the
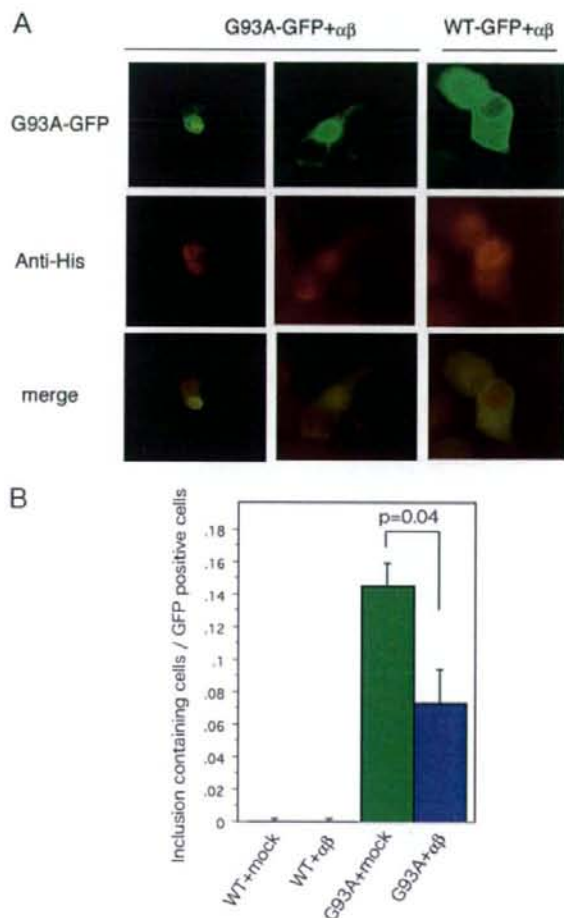

FIGURE 5. **Co-localization of mutant SOD1 and *M. mazei* proteasomes.** *A*, Neuro2a cells grown on glass coverslips were co-transfected with SOD1^{WT}-GFP or SOD1^{G93A}-GFP and Mm proteasome α- and His-tagged β-subunit. 48 h after transfection, cells were fixed, blocked, and incubated with anti-His antibody for 24 h. After washing, samples were incubated with Alexa-546-conjugated anti-mouse antibody. SOD1^{G93A} and the Mm proteasome co-localized and formed aggregates together. *WT*, wild-type SOD1; *G93A*, SOD1^{G93A}. *B*, the percentages of aggregate-positive cells among the GFP-positive cells were determined. SOD1^{G93A} aggregates were significantly reduced when co-expressed with Mm proteasome $\alpha\beta$. Error bars, S.D. ($n = 3$). Statistical analyses were carried out by Mann-Whitney's *U* test.

activation of caspase-3/7, resulting in reductions of cellular toxicities of SOD1 proteins (Fig. 4*D*). These results show that Mm proteasome $\alpha\beta$ has a protective effect against the decrease in cellular viability evoked by mutant SOD1.

M. mazei Proteasome Co-localizes with Aggregates Formed by Mutant SOD1—In the assembly process of the archaeal proteasome, α-subunit assembly is required for β-subunit incorporation into the proteasome (20), and since the anti-His-stained β-subunit is restricted largely to that incorporated into the Mm proteasome (Fig. 1*E*), we used anti-His staining to localize the transfected proteasome in Neuro2a cells. GFP-tagged wild-type and G93A mutant SOD1 vectors were transfected along with Mm proteasome $\alpha\beta$ into Neuro2a cells, which were then fixed and immunostained with anti-His antibody. Fig. 5*A* shows that

- 236 -